Effect of Sulfur and Oxygen on Weld Penetration of High-Purity Austenitic Stainless Steels

D.K. Aidun and S.A. Martin

Convective flow during arc welding depends upon the surface tension gradient ($d\gamma/dT$, Marangoni flow), buoyancy, arc drag force, electromagnetic force, shielding gas, and the viscosity of the melt. The Marangoni and the buoyancy-driven flow are the major factors in controlling weld penetration in ferrous alloys, especially austenitic stainless steels such as 304 and 316. Small variations in the concentration of surfactants, such as sulfur and oxygen, in stainless steels cause significant changes in the weld penetration and depth/width (D/W) ratio of the fusion zone. Gas-tungsten arc (GTA) welds were done on low- and high-sulfur 304 and 316 heats using pure argon and argon/oxygen shielding gases. Also, laser beam (LB) welds were done on the 304 and 316 heats using pure argon as the shielding gas. Increase in the sulfur content decreased the D/W ratio for the GTA 304 welds using pure argon, but for the case of LB 304 welds the results were the opposite. For the GTA 316 welds and LB 316 welds, increase in sulfur increased the D/W ratio of the fusion zone. Oxygen increased the D/W ratio of both the 304 and 316 GTA welds.

Keywords gas-tungsten arc welding, shielding gases, stainless steel, type 304, type 316, welding

1. Introduction

In the mechanized autogenous gas-tungsten arc (GTA) welding of stainless steel, it is customary to select the welding parameters to produce, after a specified number of passes, a full-penetration joint. On occasion, certain stainless steels which meet the required material specifications, such as 304 and 316, have been found to produce joints which differ significantly from the norm with respect to weld penetration and geometry. These differences can be caused by subtle changes in the amounts of certain elements contained in the stainless steels (Ref 1-11).

Elements can be classified into three groups: surface-active elements, those reacting strongly with surface-active elements, and those having insignificant influence on the surface tension of the melt.

Small differences in the concentration of surface-active elements (surfactant), such as sulfur and oxygen, cause substantial changes in the surface tension (γ) and surface tension gradient ($d\gamma/dT$) of ferrous alloys. Depending upon the sign of the $d\gamma/dT$, the fluid flow can be inward, increasing the depth/width (D/W) ratio, or outward, decreasing the D/W ratio. However, besides this Marangoni flow that is caused by soluble surface-active elements that change the entropy of the system, the electromagnetic (Lorentz) and gravitational forces also have a significant effect on the weld penetration of stainless steels.

This experimental research work was conducted to better understand the role of sulfur and oxygen on the weld penetration of high-purity 304 and 316 stainless steels.

D.K. Aidun and **S.A. Martin**, Clarkson University, Potsdam NY 13699-5725, USA.

2. Review

One difficulty with welding austenitic stainless steels is that identical changes in weld parameters can cause different, or even opposite, effects on the weld penetration of different stainless steels with similar compositions. This effect is caused by subtle differences in the compositions which alter the flow pattern in the molten weld pool.

The theory proposed by Heiple and Roper (Ref 1) states that the major driving force of the convective flow in a molten weld pool is caused by a surface tension gradient. The surface tension of the liquid metal is dependent upon its temperature, and therefore dependent upon the distance away from the center of the weld pool, since a molten weld pool has a radial temperature gradient such that the highest temperature is directly beneath the tip of the electrode, and the lowest is at the solid-liquid interface. The combination of the dependence of the surface tension (γ) on the temperature (T) and the presence of a temperature gradient causes a surface tension gradient ($d\gamma/dT$).

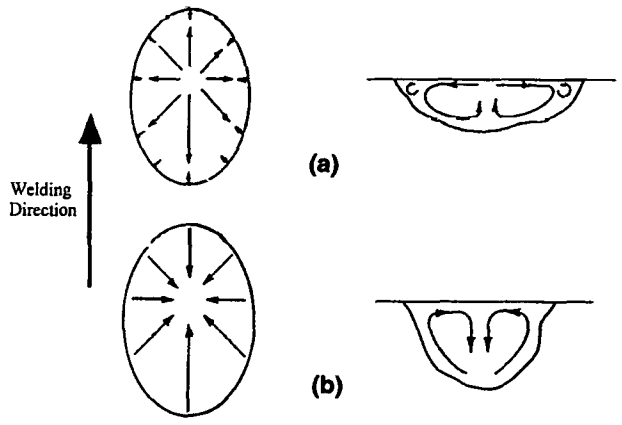

Fig. 1 Fluid flow pattern in molten weld pool. (a) Negative surface tension gradient. (b) Positive surface tension gradient. Source: Ref 1

The direction of the flow in the weld pool caused by the surface tension gradient depends upon the sign of the gradient. Flow in the molten weld pool is outward if the sign of the gradient is negative, as is the case with most pure metals (Fig. 1a). Conversely, if the gradient is positive, the flow is inward, which increases the D/W ratio (Fig. 1b).

The elements which are considered surface-active (surfactant) are sulfur, oxygen (Ref 2-4), selenium, and tellurium (Ref 4). Takeuchi et al. (Ref 11) have shown that bismuth behaves as a surfactant in austenitic stainless steel. The addition of bismuth results in a positive $d\gamma/dT$ and causes the surface tension to increase with increasing heat input. Other elements which also affect the flow by interacting with the surfactant are aluminum, silicon, manganese (Ref 2, 3), and calcium (Ref 2, 5).

The papers surveyed (Ref 1-8) suggest that sulfur added to the metal will cause an inward flow, and consequently a deeper-penetrating weld. Walsh and Savage (Ref 8) hypothesized that this is due to formation of FeS at the surface of the weld pool, which has a significantly lower surface tension than pure iron. The critical level of sulfur in the weld pool (the point where the $d\gamma/dT$ changes from negative to positive) was said to be 60 ppm by Mills and Keene (Ref 2). An optimum range of sulfur content for type 304 was suggested by Pollard (Ref 3) to be 0.010 to 0.015 wt%, which gives adequate penetration and hot workability. Dyson (Ref 9) determined the effect of sulfur on the surface tension of iron at 1600 °C, as shown in Fig. 2. Mills et al. (Ref 10) determined the relationship between sulfur content and the $d\gamma/dT$ of 304 and 316, which is shown in Fig. 3. It is conceivable that the spread of the data in Fig. 3 is due to interaction of other elements with sulfur and that the effect of the interaction is temperature dependent.

According to Heiple and Roper (Ref 1) and Shahab et al. (Ref 4), oxygen is a surface-active element with a slightly lesser effect on the $d\gamma/dT$ than sulfur. The effect of oxygen, however, can be negated by the addition of deoxidants such as aluminum, silicon, manganese, and calcium. The first three deoxidants are commonly found in 304 and 316 stainless steels. Aluminum is not a surfactant, so it has no direct effect on the $d\gamma/dT$, but it does have an indirect effect on it. It reacts with the oxygen in the alloy, and since oxygen is not free to affect the $d\gamma/dT$, the net effect of the aluminum is to decrease the D/W ratio (Ref 1-3). Pollard (Ref 3) suggests that small addition of silicon increases the weld penetration by decreasing the viscosity of the molten weld metal. It has been hypothesized that aluminum and silicon, when added together in concentrations above 0.5 wt% to the alloy, react in combination with any existing oxygen to form $MnSiO_3$ (Ref 1, 2). These particles float to the surface and have beneficial effects on the arc charac-

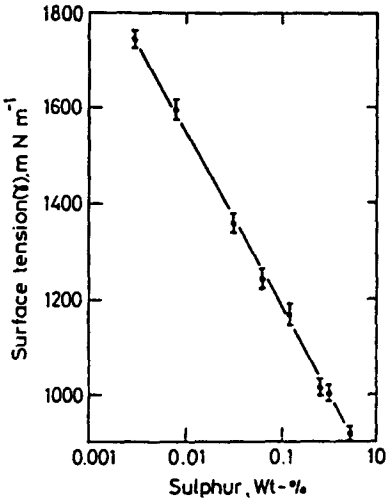

Fig. 2 Effect of sulfur on surface tension of iron at 1600 °C. Source: Ref 9

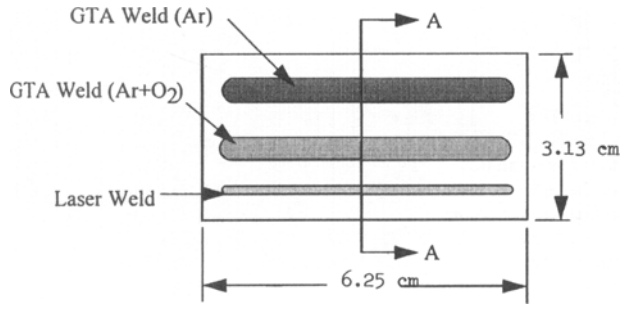

Fig. 4 Bead-on-plate coupon configuration and weld orientations

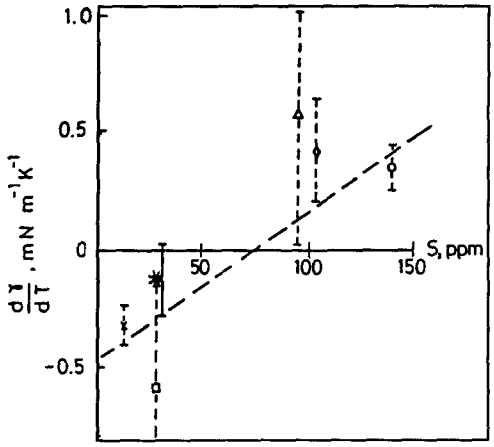

Fig. 3 Dependence of the surface tension gradient on the sulfur content of 304 and 316 stainless steels. Source: Ref 10

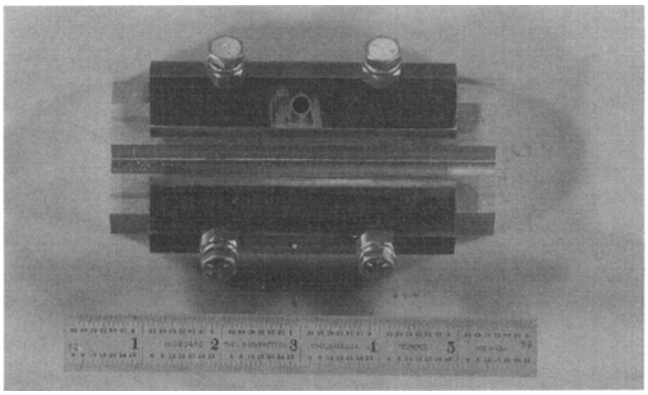

Fig. 5 Fixture used for gas-tungsten arc square butt welds

teristics, thereby increasing the heat input (Ref 2) and the weld penetration. Calcium is a reactive element that tends to cause poor penetration by reacting with free oxygen and sulfur in the molten weld pool (Ref 5). According to Mills (Ref 2), less than 10 ppm Ca reduces the levels of oxygen and sulfur to the point that the $d\gamma/dT$ becomes negative and reduces weld penetration.

3. Experimental Procedure

Five different heats of austenitic stainless steels were used for this project. Their compositions are shown in Table 1. The abbreviations LS, HS, and C stand for low-sulfur, high-sulfur, and commercial grade, respectively.

Bead-on-plate welds were done on all five alloys using GTA and laser beam (LB) welding processes to study the resulting weld D/W ratio. Two different argon-based shielding gases (commercial Ar and 99Ar-$1O_2$) were used to determine the effect of additional surfactant (oxygen) in the molten weld pool. All of the weld beads were done on one welding coupon with the weld orientations as shown in Fig. 4. The GTA and LB welding parameters are shown in Tables 2 and 3, respectively. The depth and width of the welds were measured using a digital image processing system which allowed the investigator to measure the size of the fusion zone with approximate error of ±0.025 mm.

In addition, GTA butt welds were performed between similar and dissimilar stainless steel heats. The different combinations of specimens welded are shown in Table 4 and the welding parameters used are shown in Table 5. The fixture used for the butt welds and the configuration of the coupons are shown in Fig. 5 and 6, respectively.

4. Results and Discussion

Two sets of bead-on-plate welds were performed on the three heats of 304 and the two heats of 316 using a GTA welding process. Figure 7 shows the cross sections of the weld done on 304 heats with commercial-grade argon shielding gas, while Fig. 8 shows the same for the welds done with 99Ar-$1O_2$ shielding gas. Figures 9 and 10 show the effect of sulfur and

Table 1 Compositions of austenitic stainless steels (wt%)

Type/thickness	C	Si	Mn	P	S	Cr	Ni	Mo	Cr_{eq}/Ni_{eq}(a)
304LS/3 mm	0.1	0.6	1.1	0.03	0.003	18.09	8.45	...	1.76
304HS/3 mm	0.1	0.4	0.9	0.02	0.008	18.29	8.40	...	1.78
304C/3 mm	0.1	1.0	2.0	0.05	0.030	18/20	8/12	...	1.53
316LS/2 mm	0.1	0.5	0.8	0.02	0.001	17.58	11.74	2.07	1.50
316HS/2 mm	0.1	0.5	0.8	0.03	0.006	17.55	11.83	2.25	1.46

(a) Cr_{eq}, %Cr + %Mo + 1.5 × %Si + 0.5 × %Nb; Ni_{eq}, %Ni + 30 × %C + 0.5 × %Mn

Table 2 Gas-tungsten arc welding parameters for bead-on-plate welds

Parameter	Value
Current, A	120
Voltage, V	14
Travel speed, cm/min	37 (type 304) 50 (type 316)
Shielding gas	Commercial Ar and 99Ar-$1O_2$
Gas flow rate, cm^3/min	450
Arc length, cm	0.1
Stick out, cm	0.2
Electrode type/size	W-2ThO_2/0.15 cm
Polarity	DC-EN

Table 3 Laser beam welding parameters for bead-on-plate welds

Parameter	Value
Laser type	CO_2
Power, W	1125
Duty cycle, %	100
Travel speed, cm/min	90 (type 304) 337 (type 316)
Shielding gas	Commercial Ar
Gas pressure, MPa	0.28
Lens focal length, cm	6.2
Lens diameter, cm	2.7
Focal position, cm	0.0
Nozzle diameter, cm	0.7

Table 4 Combinations of gas-tungsten arc square butt welds

First specimen	Type of specimen welded
304LS	304LS
304HS	304HS
304C	304C
304LS	304HS
304LS	304C
304HS	304C
316LS	316LS
316HS	316HS
316LS	316HS

Table 5 Gas-tungsten arc welding parameters for butt welds

Parameter	Value
Current, A	120
Voltage, V	14
Travel speed, cm/min	37
Shielding gas	Commercial Ar
Gas flow rate, cm^3/min	450
Arc length, cm	0.1
Stick out, cm	0.2
Electrode type/size	W-2ThO_2/0.15 cm
Polarity	DC-EN

oxygen, respectively, on the weld penetration of 316 heats. Table 6 shows the effect of sulfur and oxygen on the D/W ratio of the 304 and 316 heats.

The data for 316 heats suggest that high sulfur content and oxygen content result in a higher D/W ratio. These data agree with previously published work (Ref 1-8). However, the effect of sulfur on the D/W ratio of 304 heats suggests otherwise. It is believed that in the 304C heat the amount of Mn + Si (~3 wt%) is responsible for the low D/W ratio. By addition of oxygen the D/W ratio for 304 heats increases, but the D/W ratio of 304C is still the lowest due to the higher Mn + Si content. This result also agrees with previous work.

In Table 6 the LB welds done on 316 heats show the same results regarding the D/W ratio, but for the case of 304 heats the D/W ratio results are not the same as for GTA welds. In this case, as the sulfur content of the 304 increased, the D/W ratio also increased. Although chemical analysis was not done on the LB welds, it is conceivable that due to the keyhole nature of LB welding, vaporization of manganese and/or silicon occurred in the weld pool, altering the Mn + Si content of the fusion zone. Macrographs of the 304 and 316 LB welds are shown in Fig. 11 and 12, respectively.

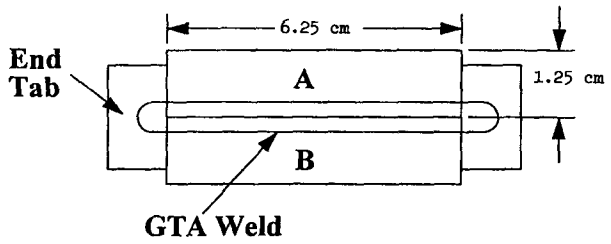

Fig. 6 Configuration of coupons for gas-tungsten arc square butt welds

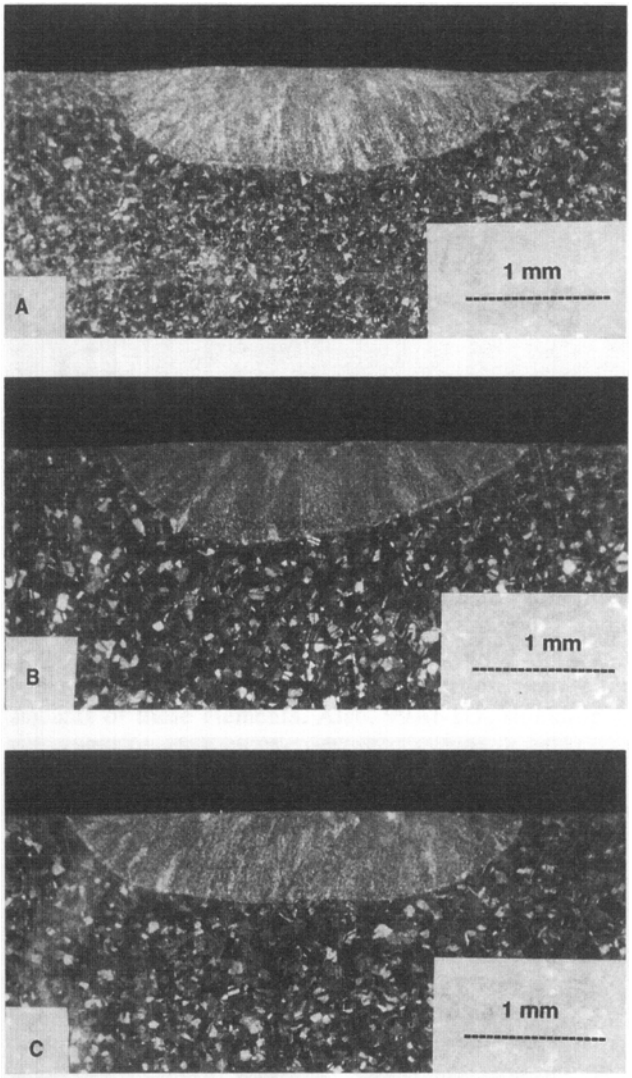

Fig. 7 Gas-tungsten arc bead-on-plate welds for (a) 304LS, (b) 304HS, and (c) 304C, using argon gas

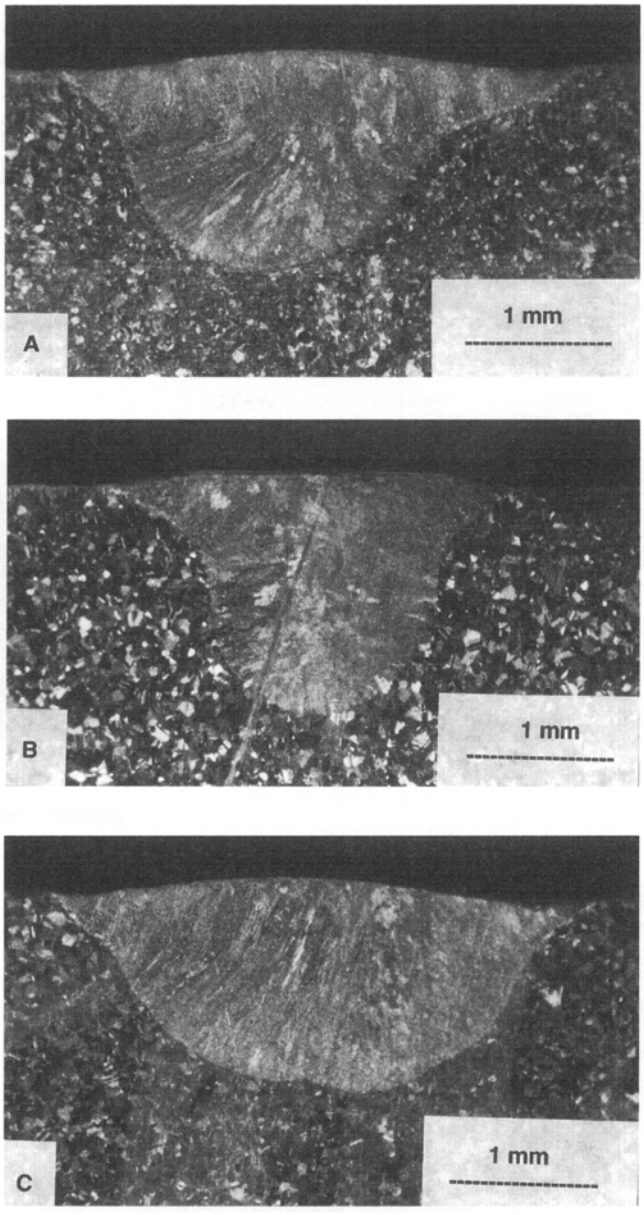

Fig. 8 Gas-tungsten arc bead-on-plate welds for (a) 304LS, (b) 304HS, and (c) 304C, using 99Ar-1O_2 gas

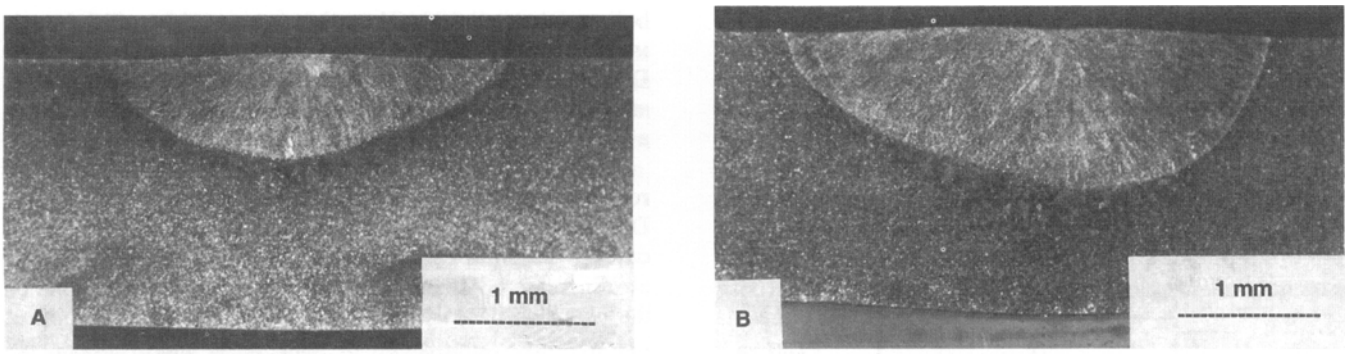

Fig. 9 316LS gas-tungsten arc bead-on-plate welds. (a) Argon gas. (b) 99Ar-1O_2 gas

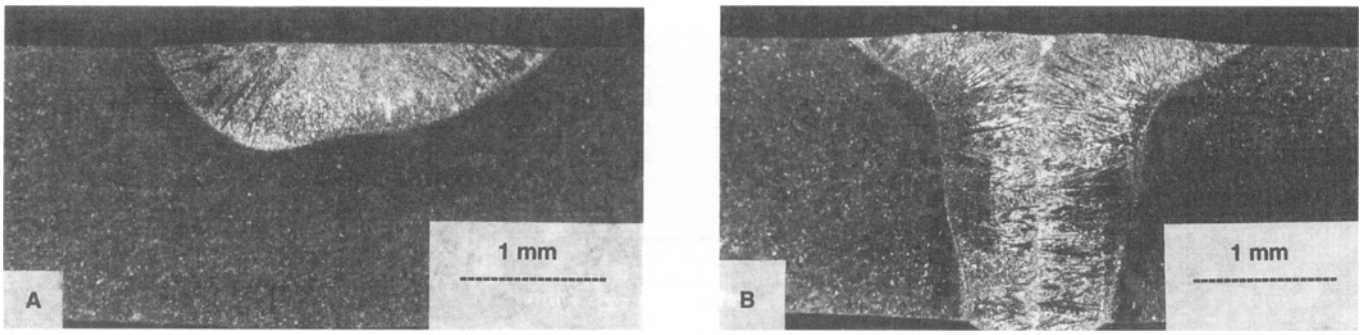

Fig. 10 316HS gas-tungsten arc bead-on-plate welds. (a) Argon gas. (b) 99Ar-1O_2 gas

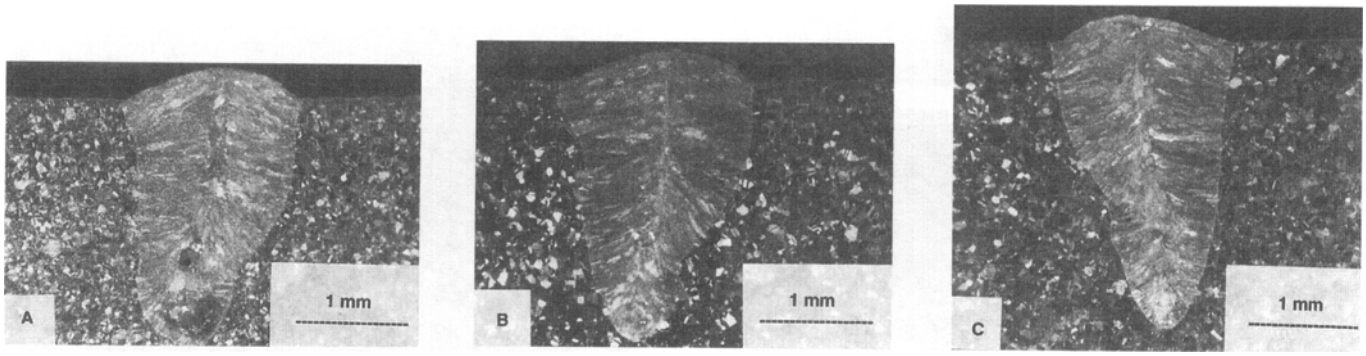

Fig. 11 Laser beam bead-on-plate welds for (a) 304LS, (b) 304HS, and (c) 304C, using argon gas

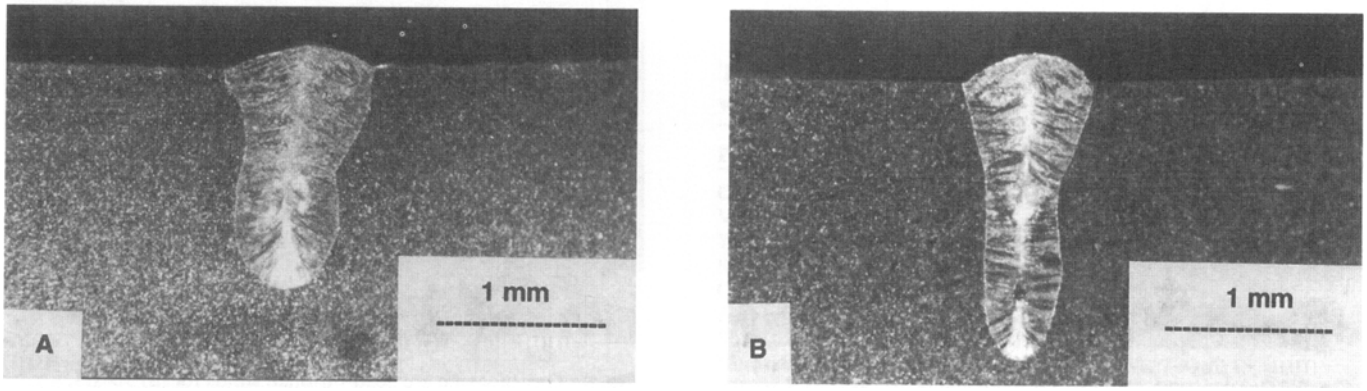

Fig. 12 Laser beam bead-on-plate welds for (a) 316LS and (b) 316HS, using argon gas

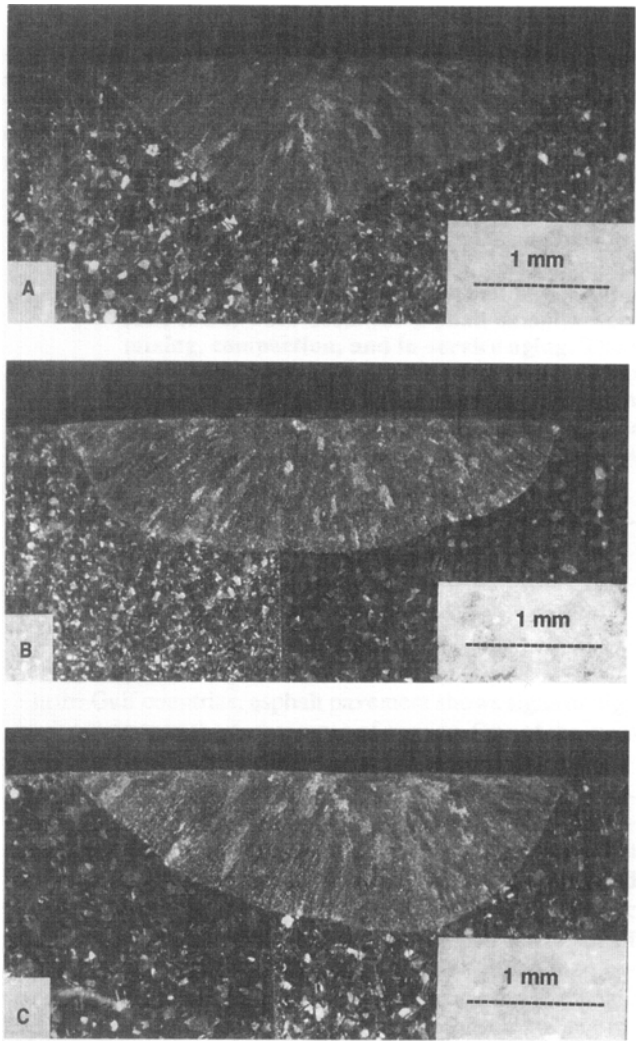

Fig. 13 Gas-tungsten arc square butt welds between (a) 304HS/304LS, (b) 304LS/304C, and (c) 304C/304HS, using argon gas

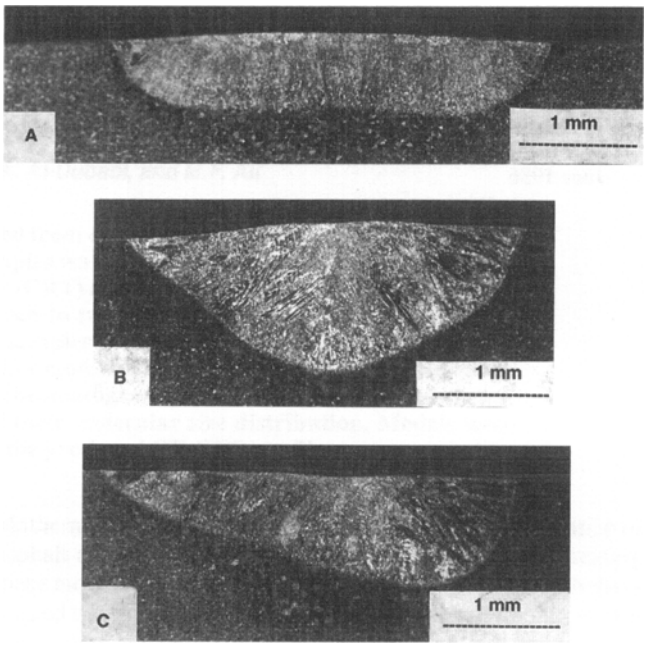

Fig. 14 Gas-tungsten arc square butt welds between (a) 316LS/316LS, (b) 316HS/316HS, and (c) 316LS/316HS, using argon gas

Table 6 Fusion zone depth/width (D/W) ratios of the bead-on-plate welds

Material	GTAW D/W (Ar)	GTAW D/W (99Ar-1O_2)	LBW D/W (Ar)
304LS	0.249	0.392	1.35
304HS	0.246	0.565	1.44
304C	0.202	0.368	1.52
316LS	0.259	0.317	1.45
316HS	0.270	Full penetration	2.05

GTAW, gas tungsten arc weld; LBW, laser beam weld

Based on these experiments, the oxygen content has a greater effect on the weld penetration than sulfur does, which is opposite to what was previously thought. It should be noted that it is the amounts of soluble sulfur and oxygen in the weld which affect the weld penetration, not the total amounts of these elements. Also, 99Ar-1O_2 shielding gas produces a hotter GTA than pure argon, resulting in a higher D/W ratio.

Figure 13 shows the cross-sectional view of the GTA butt welds for 304 heats, and Fig. 14 shows the same for 316 heats. Figures 13(a) and (c) illustrate the formation of a nonaxisymmetric weld pool resulting from diffusocapillary and thermocapillary action due to the different sulfur contents of the 304 heats (Ref 2). However, for the case of 316 heats (Fig. 14c), the effect is opposite and the flow is directed toward 316 with higher sulfur content. By examining Fig. 14 qualitatively it is reasonable to place the higher D/W on the side of the 316HS rather than the side of 316LS.

Based on the above data, the results do confirm the effect of surfactant on the weld penetration. However, it is important to understand that minor changes in the composition, welding parameters, welding process, and shielding gas do alter the weld penetration, at least in 304 and 316 stainless steels.

References

1. C. Heiple and J. Roper, Mechanism for Minor Element Effect on GTA Fusion Zone Geometry, *Weld. J.*, April 1982
2. K.C. Mills and B.J. Keene, Factors Affecting Variable Penetration, *Int. Mater. Rev.*, Vol 35 (No. 4), 1990
3. B. Pollard, The Effects of Minor Elements on the Welding Characteristics of Stainless Steel, *Weld. J.*, Sept 1988
4. A. Shahab, S.K. Marya, F. Le Maitre, and J. Binard, "Effect of Sulfur on the GTA Welding of a Stainless Steel," paper presented at the International Conference on Joining of Materials, (Helsingor, Denmark), 1991
5. A. Okada and J. Nakamura, Control of Trace Elements Effect in TIG Welding of Thin Plate, Report, National Research Institute for Metals, Tokyo to VAMAS, Weld Characteristics, NPL, Teddington, 5 Dec 1988
6. D.W. Walsh and W.F. Savage, Autogenous GTA Weldments—Bead Geometry Variation due to Minor Elements, *Weld. J.*, Feb 1985

7. T. Zacharia, S.A. David, J.M. Vitek, and T. Debroy, Weld Pool Development during GTA and Laser Beam Welding of Type 304 Stainless Steel, Part II: Experimental Correlation, *Weld. J.*, Dec 1989
8. P. Burgardt and C.R. Heiple, Interaction between Impurities and Welding Variables in Determining GTA Weld Shape, *Weld. J.*, June 1986
9. B. Dyson, *Trans. AIME,* 1963, p 227
10. K.C. Mills, B.J. Keene, R.F. Brooks, and A. Olusanya, Paper R, *Proc. Centenary Conf. Metallurgy Dept.*, University of Strathclyde, Glasgow, June 1984
11. Y. Takeuchi, R. Takagi, and T. Shinoda, Effect of Bismuth on Weld Joint Penetration in Austenitic Stainless Steel, *Weld. J.*, Aug 1992